Journal of Alloys and Compounds 505 (2010) 11–16

Contents lists available at ScienceDirect

Journal of Alloys and Compounds

journal homepage: www.elsevier.com/locate/jallcom

High magnetic field study of the anisotropy and neutron diffraction investigation of the crystal and magnetic structure of $YCo_{4.5}Ge_{0.5}$

C.V. Colin [a,*], O. Isnard [a], M. Guillot [b]

[a] Institut Néel, CNRS/Université Joseph Fourier, B.P. 166, 38042 Grenoble Cedex 9, France
[b] Laboratoire National des Champs Magnétique Intenses, CNRS/Université Joseph Fourier B.P. 166, 38042 Grenoble Cedex 9, France

ARTICLE INFO

Article history:
Received 15 April 2010
Accepted 7 June 2010
Available online 12 June 2010

PACS:
75.25.−j
75.30.Gw
75.50.Cc

Keywords:
Intermetallic compound
Magnetic properties
Anisotropy

ABSTRACT

The solubility limit of Ge in the $YCo_{5-x}Ge_x$ structure is shown to be close to one Ge atom per formula unit by combining diffraction techniques and electron microscopy. The evolution of the crystal structure of the $YCo_{4.5}Ge_{0.5}$ compound is studied by X-ray and neutron diffraction experiments. A preferential substitution scheme is observed, the Ge atom being preferentially located on the Co 3g positions. Powder neutron diffraction results shows that the Co magnetic moments are significantly reduced by the presence of Ge in the crystal structure. The intrinsic magnetic properties such as the saturation magnetization and the magnetocrystalline anisotropy parameters are determined at 4.2 and 300 K from a fit of the isothermal magnetization curves measured in applied field up to 23 T. Ge for Co substitution induces a reduction of the first order anisotropy parameter. The large magnetocrystalline anisotropy found for $YCo_{4.5}Ge_{0.5}$ is not much reduced upon heating from 4 to 300 K. The results are compared and commented in the light of that reported earlier for YCo_5 and other homologues such as YCo_4Al or YCo_4Ga.

1. Introduction

Since their discovery in 1947 ($CeCo_5$), the hexagonal RCo_5 intermetallics have been intensively studied from the fundamental viewpoint but also for their potential applications [1–4]. The RCo_5 compounds have been widely used as permanent magnets because of their excellent magnetic properties: high Curie temperature (T_C), large magnetocrystalline anisotropy (MCA), and important saturation magnetization (M_s). These performances are due to the combination of the complementary characteristics of 3*d*-itinerant and 4*f*-localized magnetism of Co and R, respectively. The RCo_5 compounds crystallize in the hexagonal $CaCu_5$ type structure with *P*6/*mmm* space group. Materials with this hexagonal structure were especially investigated for possible extremely high magnetocrystalline anisotropy. In spite of their relatively old discovery the RCo_5 type compounds are still attracting much interest nowadays from both the experimental and theoretical point of view in order to deeper understand their intrinsic physical properties such as the magnetoelastic properties [5,6]; the exchange interactions [7,8]; the electronic structure [9,10] or the magnetocrystalline anisotropy [11,12].

The $RCo_{5-x}M_x$ compounds, where R is yttrium or a rare earth, have been extensively studied both because their crystalline structure derives from the technologically important RCo_5 structures and because their magnetic properties and, more specifically, their magnetic anisotropy, strongly depend upon the metalloid element M content *x* [13–16]. In particular, the effects of the substitution of Al, Ga or Si or B for Co in the RCo_5 (R = Y, Pr, Tb and Dy) compounds have been discussed in previous studies [15–24]. Here, we report on the influence of the Ge for Co substitution in the RCo_5 structure based on the investigation of the $YGo_{5-x}Ge_x$ system. The phase stability will be probed by combining X-ray diffraction, electron microscopy investigation and energy dispersive X-ray microanalysis. Then we present results of neutron diffraction investigations performed on $YCo_{4.5}Ge_{0.5}$ compounds between 2 and 300 K to establish both the Ge substitution scheme and the magnetic structure of the $YCo_{4.5}Ge_{0.5}$ phase. In addition to neutron diffraction experiments, high magnetic field measurements are performed to investigate the magnetocrystalline anisotropy of the $YCo_{4.5}Ge_{0.5}$ phase and deduce the influence of Ge for Co substitution on the anisotropy of the Co sublattice.

2. Experimental

2.1. Synthesis and sample preparation

The polycrystalline samples of $YCo_{5-x}Ge_x$ studied herein were prepared from high purity elements better than 99.95% for elemental Co, Ge and Y, respectively, using a high frequency furnace under purified Ar atmosphere. The samples were

* Corresponding author.
E-mail address: claire.colin@grenoble.cnrs.fr (C.V. Colin).

0925-8388/$ – see front matter © 2010 Elsevier B.V. All rights reserved.
doi:10.1016/j.jallcom.2010.06.025

then quenched from the melt in the water cooled copper crucible. The purity of the phases has been characterized by X-ray diffraction and electron microscopy analyses see below. Field oriented samples were prepared by solidifying, at room temperature, the mixture of epoxy resin and of the powdered specimen in a magnetic field of c.a. 0.6 T. Prior to the orientation, the samples were powdered and then sieved down to a particle size smaller than 30 μm.

2.2. X-ray diffractometry and electronic microscopy

The phase purity of the samples was checked by means of X-ray diffraction using a $\theta/2\theta$ diffractometer and Co $K_{\alpha 1}$ radiation 1.789 Å. Experiments have also been performed on the powder sample previously oriented under an applied magnetic field, thus enabling to determine the easy magnetization direction of the sample. The alloy purity has been checked by using a JEOL 840A scanning electron microscope equipped with an KEVEX energy dispersive X-ray EDX microprobe.

2.3. Neutron diffraction

Neutron diffraction experiments were carried out at the high flux reactor of the Institut Laue Langevin (Grenoble, France) using the high-resolution two-axis powder diffractometer D1A operating with a take off angle of 122° from the monochromator. The measurements were carried out at a wavelength of 1.91 Å selected by the (1 1 5) reflection of a Ge monochromator. The diffraction pattern at room temperature (300 K) was measured over the 2θ range from 2° to 160° with a step size of 0.05°. Further neutron diffraction patterns as function of temperature were obtained using the high flux powder diffractometer D1B (French CNRS-CRG instrument). The two-axis D1B powder diffractometer used for this work was equipped with a large one dimensional 400 cell curved detector which recorded the diffraction pattern over a 2θ range of 80°. The neutron wavelength of 2.52 Å was selected by the (0 0 2) reflection of a pyrolitic graphite monochromator and the 2θ step was 0.2°. All powder neutron diffraction data were analyzed using the Rietveld line profile technique implemented with the program FULLPROF [25]. This program permits multiphase and magnetic structure refinement of each of the components present. A pseudo-Voigt type peak shape function was used in the refinements and, in the case of the D1B data, the peak shape was very close to pure Gaussian. For the very low angle Bragg reflections, an asymmetry parameter has been used to mimic the known instrumental asymmetry of the D1A diffractometer. The coherent neutron scattering lengths were $b_{Ge} = 0.8185 \times 10^{-12}$, $b_{Co} = 0.249 \times 10^{-12}$ cm, and $b_Y = 0.775 \times 10^{-12}$ for Ge, Co and Y, respectively [26].

A full description of the Rietveld method used in this article as well as the definition of the agreement factors can be found elsewhere [27].

2.4. Magnetic measurements

The magnetic ordering temperature has been determined with a Faraday type balance at heating and cooling rates of 5 K/min. A sample of c.a. 50–100 mg was sealed under vacuum in a small silica tube in order to prevent oxidisation of the sample during heating. The magnetization measurement of $YCo_{4.5}Ge_{0.5}$ was performed at 4.2 and 295 K using the extraction method [28] in applied fields of zero to 23 T. The magnetic field was produced by a water cooled resistive magnet at the LNCMI high magnetic field laboratory in Grenoble, France.

3. Results and discussion

3.1. Crystal structure

The YCo_5 phase crystallize in the hexagonal $CaCu_5$-type structure with *P*6/*mmm* space group. Fig. 1 presents this structure which comprises one site for Ca (1a) and two different crystallographic positions for Cu (2c and 3g). The 2c site lies in the same plane as the 1a site and the 3g position is situated between the layers containing the 2c and the 1a sites. The RCo_5 structure is isotypic to the $CaCu_5$ one where R and Co atoms are situated in the Ca and Cu positions, respectively.

X-ray diffraction analysis shows that this $CaCu_5$-type structure of the starting YCo_5 is preserved until the Ge for Co substitution equal to 1. The $YCo_{4.5}Ge_{0.5}$ and YCo_4Ge compounds are found to be nearly single phase whereas the substitution of more Ge leads to the appearance of a second Ge rich phase. Indeed traces of impurity phase of $Y_2(Co/Ge)_7$ can be observed in Fig. 2. Consequently the solubility limit of Ge in YCo_5 is supposed to be between 1 and 1.5 Ge atom per formula unit. This value is comparable to that of Si solubility limit reported earlier [29]. The summary of the results found by X-ray diffraction are displayed in Table 1, this includes a list of

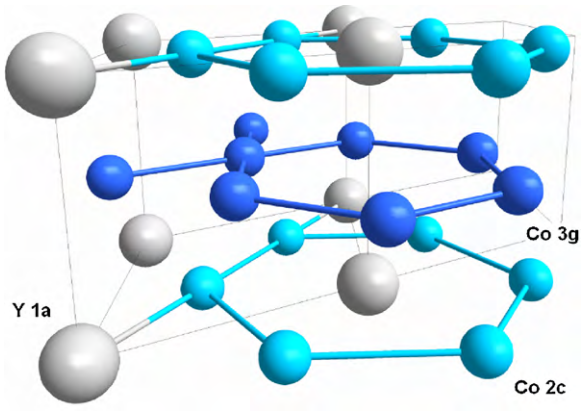

Fig. 1. The hexagonal crystal structure of YCo_5 ($CaCu_5$-type structure of *P*6/*mmm* space group). Yttrium atoms in the centre of the hexagons are represented by grey spheres, the two crystallographically non-equivalent cobalt atoms at the corners (2c site) and on the prism face centers (3g site) are represented by light-blue and dark-blue spheres. (For interpretation of the references to color in this figure legend, the reader is referred to the web version of the article.)

the phases present together with the corresponding lattice parameters deduced from least squared refinement taking into account all the observed Bragg reflections.

The lattice parameters are increasing upon Ge for Co substitution because of the larger atomic radius of Ge. This expansion of the unit cell is more pronounced along the *c*-axis than in the basal plane since the c/a ratio is increasing upon Ge substitution. The analysis by scanning electron microscopy (SEM) confirms the good homogeneity and stoichiometry of the $YCo_{4.5}Ge_{0.5}$ and YCo_4Ge compounds. More phases can be observed for richer Ge content. For instance, Fig. 3 shows the SEM picture of $YCo_{3.5}Ge_{1.5}$ alloy. As can be seen from this electron micrograph, coexistence of different phases is observed. A bright one corresponding to a larger electronic concentration and the $CaCu_5$ type phase which appears darker. EDX microprobe analysis reveals that this minor impurity phase contains all the three elements Ge, Co and Y. The inspection of the X-ray microanalysis reveals the presence of YCo_2Ge_2 for the non-single-phase the $YCo_{5-x}Ge_x$ materials with $x = 1.5$ and 2. It is worth to note that the main phase is the $CaCu_5$ type with traces of YCo_2Ge_2 as impurity whereas for the YCo_3Ge_2 alloy the majority phase is the YCo_2Ge_2 one. In addition to the estimation of the atomic content of the different phases extracted from the EDX microanalysis,

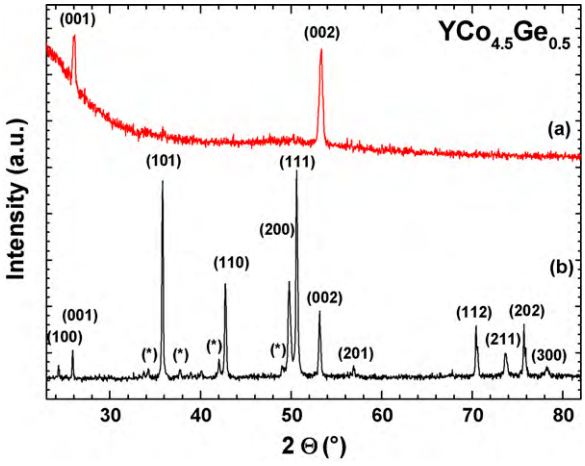

Fig. 2. XRD patterns recorded on a field-oriented sample (a) and on a free powder (b) of $YCo_{4.5}Ge_{0.5}$ at room temperature ($\lambda = 1.79030$ Å). The Y_2Co_7 minority phase contribution is indicated with stars.

Table 1
Structure types and room temperature lattice parameters of the phases observed in the $YCo_{5-x}Ge_x$ alloys as determined by X-ray powder diffraction.

Composition	Phases and structure type	Space group	a (Å)	c (Å)	c/a	Cell vol. (Å^3)
YCo_5 [4]	YCo_5	$P6/mmm$	4.937	3.978	0.806	83.970
$YCo_{4.5}Ge_{0.5}$	YCo_5	$P6/mmm$	4.956(1)	4.002(1)	0.807	85.137
YCo_4Ge	YCo_5	$P6/mmm$	4.943(9)	4.018(7)	0.812	85.03
$YCo_{3.5}Ge_{1.5}$	YCo_5	$P6/mmm$	4.993(2)	3.978(2)	0.797	85.913
	YCo_2Ge_2	$I4/mmm$	3.9730(2)	10.0925(6)	–	158.215
YCo_3Ge_2	YCo_2Ge_2	$I4/mmm$	3.9730(2)	10.0925(6)	–	158.215

Fig. 3. SEM picture of $YCo_{3.5}Ge_{1.5}$ compound. Three different phases can be observed. Energy dispersive X-ray analysis give a stoichiometry around YCo_2Ge_2 for phases 1 and 2 whereas phase 3 has a stoichiometry close to $YCo_{3.5}Ge_{1.5}$.

the inspection of the X-ray diagrams confirms the existence of the phases discussed above in the $YCo_{5-x}Ge_x$ materials.

A precise determination of the Ge location in the $CaCu_5$-type structure was completed by neutron powder diffraction investigations. From the neutron diffraction experiments carried out at room temperature on the high resolution powder diffractometer D1A (Fig. 4) it is found that the Ge atoms occupy preferentially the 3g crystallographic site of the $CaCu_5$ structure (Table 2). Previous

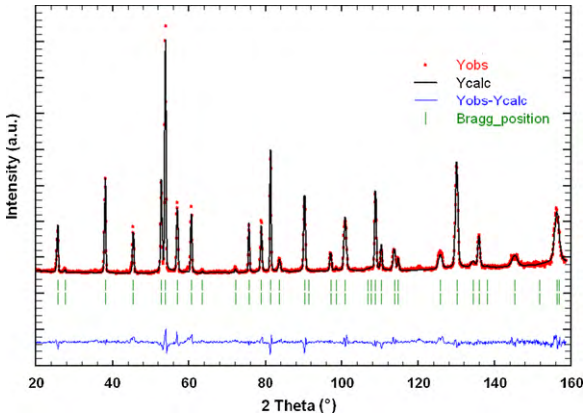

Fig. 4. The powder neutron diffraction pattern of $YCo_{4.5}Ge_{0.5}$ obtained at room temperature on the D1A high resolution diffractometer (λ = 1.91 Å). The points represent the experimental data and the solid line is the result of the Rietveld profile analysis. The difference between the experimental data and the calculated pattern is plotted on the same scale in the lowest part of the figure. In between, the first and second rows of vertical lines refer to the magnetic and nuclear contributions to the diffraction pattern.

Table 2
Rietveld refinement results of the $YCo_{4.5}Ge_{0.5}$ powder neutron diffraction patterns recorded at 10 and 300 K.

T (K)	10	300
Instrument	D1B	D1A
λ (Å)	2.520(6)	1.910 (1)
Space group	$P6/mmm$	$P6/mmm$
a (Å)	4.936(6)	4.952(2)
c (Å)	3.993(6)	4.001(2)
Site 2c (%Co)	95 fixed[a]	95(1)
Site 3g (%Co)	87 fixed[a]	87(1)
M_{Co}(2c) (μ_B/atom)	1.0(2)	1.1(2)
M_{Co}(3g) (μ_B/atom)	1.9(2)	2.0(2)
EMD	c-axis	c-axis
R_{Bragg}, R_{Mag} (%)	6.91, 17.6	7.03, 12.9
R_{wp} (%), χ^2	11.2, 35.1	13.5, 4.77

[a] Values fixed according to the results of the high resolution powder neutron refinement at 300 K.

neutron powder diffraction studies on the substituted $RCo_{5-x}M_x$ compounds have shown that some other metalloids (M = Al, Ga and Si) also preferentially occupy the 3g crystallographic site of the $CaCu_5$ structure [18–22,30]. It is well known that in the RCo_5 structure the easy c-axis anisotropy of the Co sublattice is found to arise from the Co 2c sites, while the 3g sites make a smaller opposite (planar) contribution. The preferential location of the non-magnetic Ge atoms on the 3g sites should reduce the 3g planar contribution to the magnetocrystalline anisotropy, thus favouring an enhancement of the overall easy c-axis magnetocrystalline anisotropy due to the Co sublattice. As can be seen from Table 2, the neutron diffraction results are in good agreement with X-ray diffraction analysis concerning the lattice parameters at 300 K. The investigation of the diffraction patterns recorded every 12 K on D1B shows that the a and the c lattice parameters slightly increases as temperature increases (Fig. 5). This behaviour is usual and linked to the atomic thermal vibration. It is remarkable that the thermal expansion of the lattice occurs mostly in the basal plane whereas the c-axis does not expand much below 200 K.

It is well known that the stability range of the heavy rare earth RCo_5 phases imposes the use of the off-stoichiometric compositions

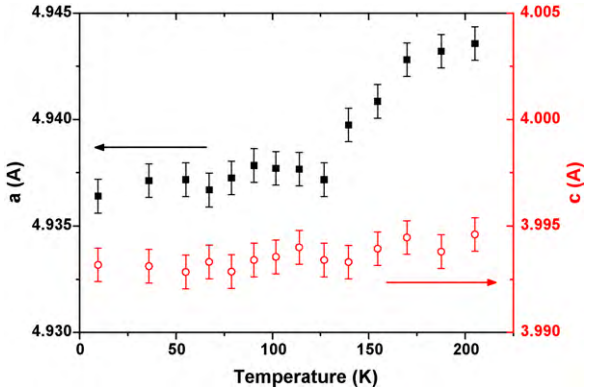

Fig. 5. Thermal evolution of the lattice parameters of $YCo_{4.5}Ge_{0.5}$. The a and c lattice parameters are plotted in close and open symbol, respectively.

Table 3
Magnetic properties of $YCo_{4.5}Ge_{0.5}$ where H_A is the magnetocrystalline anisotropy field and the other parameters are defined in Eq. (1).

Compound	T_C (K)	M_s (μ_B/f.u.)		$\mu_0 H_A$ (T)		K_1 (MJ/m^3)		K_2 (MJ/m^3)	
		4 K	300 K	4 K	300 K	4 K	300 K	4 K	300 K
YCo_5 [39,40]	945	8	7.5	18.1	13.7	7.4	5.8	−0.18	−0.36
$YCo_{4.5}Ge_{0.5}$	778(2)	5.2(1)	4.9(1)	16.5(1)	11.1(1)	2.8(7)	2.4(8)	0.7(7)	0.0(7)

described by the formula $R_{1-s}Co_{5+2s}$ [3,31], called dumbell pairs. It is worth to note that no dumbbell pairs have been found in the present study of $YCo_{4.5}Ge_{0.5}$ unlike what is usually observed for the homologue YCo_5 and other heavy rare-earth RCo_5-type phases [3].

3.2. Magnetic properties

Although the substitution of Ge for Co preserves the $CaCu_5$ structure of the RCo_5 compounds, its influences on the magnetic properties are significant. The $YCo_{4.5}Ge_{0.5}$ compound exhibits a ferromagnetic order since yttrium is nonmagnetic. The influences of Ge substitution on the magnetic Co sublattice can well be studied using $YCo_{4.5}Ge_{0.5}$ as reference compound. The saturation magnetization seriously drops down upon Ge substitution (Table 3). The dilution of the Co sublattice by Ge substitution induces a dramatic decrease of the mean Co magnetic moment μ_{Co} from 1.62 to 1.15 μ_B for YCo_5 [3,4] and $YCo_{4.5}Ge_{0.5}$, respectively. This can be explained by assuming that the two valence electrons of Ge (4s2 4p2) are partially transferred into the Co-3d band, thus reducing the Co magnetic moment. This could explain the observed reduction of the saturation magnetization M_S.

As it has been determined by thermomagnetic measurement (Fig. 6) the Ge for Co substitution leads also to a decrease of the Curie temperature from 945 to 778 K for YCo_5 and $YCo_{4.5}Ge_{0.5}$, respectively. This feature is due to the presence of Ge (non-magnetic atom), which induces a decrease of the exchange interactions in $RCo_{4.5}Ge_{0.5}$ compared with RCo_5. The p(Ge)–d(Co) hybridization might also goes together with a decrease of the strength of the Co–Co exchange interaction. Hence, the drop down of the T_C can be explained by both reductions of the number and strength of the Co–Co exchange interaction. It is worth noting that the reduction of μ_{Co} by Ge for Co substitution is similar to that obtained for Al or Ga but smaller than that obtained for the B substitution [14–19]. This indicates that the Co–B electronic hybridization is more effective than the Co–Ge one.

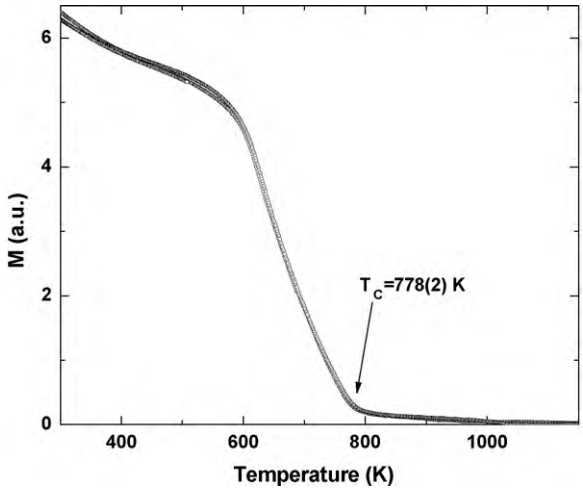

Fig. 6. Thermomagnetic measurement of $YCo_{4.5}Ge_{0.5}$.

The magnetic moments carried by each atom as determined by powder neutron diffraction analysis are listed in Table 2. In the present investigation, the sum of the refined Co magnetic moments is slightly larger than the bulk magnetization. This is a common feature since the powder neutron diffraction is essentially sensitive to the localized magnetic moments and is less sensitive to the negative polarization of the valence electrons. However, this is a powerful method to determine the direction and magnitudes of the atomic magnetic moments. We observe a rather constant contribution of the Co magnetic moments at 4 K and room temperature. The magnitude of the Co-2c magnetic moment is only about one half of those obtained on the Co-3g position. This result is true at both temperatures. This was also reported earlier for the $ErCo_{4.5}Ge_{0.5}$ isotype [32]. This difference of magnetic moments was hardly noticeable in YCo_5 where the obtained values were 1.72 and 1.77 μ_B for 2c and 3g site, respectively [33,34]. On the contrary, a large difference was observed in YCo_4B where Co magnetic moments of 1.6 and 0.6 μ_B were found to coexist. This feature is related to the change of the crystallographic structure as discussed elsewhere [23,35].

In order to determine the easy magnetization direction (EMD) at room temperature, X-ray diffraction patterns have been obtained on magnetically oriented powder. Fig. 2 shows a comparison between the diffraction patterns recorded on a free powder and that recorded on a powder aligned under a magnetic field for the $YCo_{4.5}Ge_{0.5}$ sample. X-ray diffraction pattern was recorded at room temperature for $YCo_{4.5}Ge_{0.5}$ on powder sample oriented in an applied magnetic field. In the X-ray diffraction pattern of the field-oriented sample there are only two Bragg peaks indexed as (0 0 l). Taking into account that the magnetic field is applied perpendicularly to the plane of the sample, we conclude that in $YCo_{4.5}Ge_{0.5}$ the EMD is along the *c*-axis at room temperature as in the corresponding YCo_5 reference compound. Indeed, the behaviour of the anisotropy in YCo_5 has been satisfactorily described in terms of a localized model. It has been shown that in the YCo_5 type compounds, the two inequivalent 2c and 3g sites exhibit opposite magnetocrystalline anisotropy [37,38].

It has been well established that the YCo_5 compound presents uniaxial anisotropy, with the EMD along the *c*-axis at all temperatures [39,40]. The neutron diffraction analysis of $YCo_{4.5}Ge_{0.5}$ compound shows a direction of the magnetic moments along the *c*-axis of the hexagonal structure at both 2 and 300 K, in perfect agreement with the determination established by oriented X-ray diffraction at room temperature. Furthermore, the thermomagnetic analysis performed between 300 and 1000 K for $YCo_{4.5}Ge_{0.5}$ indicates only one transition from a ferromagnetic order to a paramagnetic state. No sign of SRT has been observed unlike what was reported earlier for YCo_4B [13,14]. Thus, we can conclude that $YCo_{4.5}Ge_{0.5}$ exhibits an axial EMD up to the Curie temperature. This result is worth to be noted since in the contrary YCo_4B has been shown to exhibit a spin reorientation phenomenon indicating that its EMD is aligned along the basal plane at low temperature and along the *c*-axis above the spin reorientation [13,35,36]. This phenomenon is due to the competition between the opposite individual site anisotropies of Co atoms situated on the two inequivalent atomic sites. It is thus remarkable that in $YCo_{4.5}Ge_{0.5}$ the EMD remains along the *c*-axis of the crystal structure upon Ge for Co substitution.

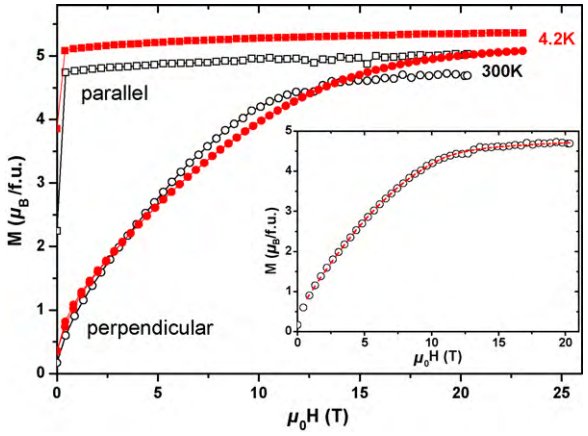

Fig. 7. Magnetization isotherms of $YCo_{4.5}Ge_{0.5}$ recorded at 4.2 (close symbol) and 300 K (open symbol) with the field applied parallel and perpendicular to the easy magnetization direction. Inset: fit of perpendicular magnetization curve at 300 K (parameters in Table 3).

As can be seen from the isothermal magnetization curves plotted in Fig. 7, the high magnetic field used here up to 23 T enables to saturate the sample in both directions, parallel and perpendicularly to the easy magnetization axis. A slightly larger anisotropy is observed at 4.2 K than at room temperature for the $YCo_{4.5}Ge_{0.5}$ compound. The anisotropy is large but smaller than the huge one reported for the YCo_5 parent compound. For an hexagonal symmetry such as for the $YCo_{4.5}Ge_{0.5}$ compound studied here, the free energy is expressed as:

$$F = K_1 \sin^2\theta + K_2 \sin^4\theta - \mu_0 H_0 (M_s + \chi_{hf}\mu_0 H_0)\cos(\theta - \theta_H) \quad (1)$$

where M_s is the spontaneous magnetization, H_0 is the internal magnetic field and χ_{hf} is the high-field differential susceptibility. The K_1 and K_2 are the anisotropy parameters. In Eq. (1), we have developed the anisotropy energy to the 4th order neglecting the higher order terms in particular the in-plane anisotropy which normally appears at the 6th order. θ denotes the angle between the magnetization direction and the c-axis of the crystal structure whereas θ_H corresponds to the angle of the magnetic field versus c-axis. Since the magnetic field is applied perpendicularly to the EMD, if the EMD is along the c-axis, θ_H value is normally 90°. However, a possible misalignment of the crystallites with respect to the direction of the applied magnetic field has been taken into account. This has been done by using au Gaussian distribution of the grains around 90° with a mean misalignment of 7°. An example of the fit is given in the inset of Fig. 7. Similar fitting procedure has been used successfully to extract the anisotropy parameters from the magnetization curves of other hard magnetic materials procedure see Ref. [41] for more details. The saturation magnetization, the anisotropic field $\mu_0 H_A$, the first K_1 and second K_2 anisotropy parameter deduced from a fit of the magnetization curve are listed in Table 3. The obtained positive sign of K_1 together with the much lower K_2 value are consistent with the existence of an easy magnetization axis along the c-axis of the crystal structure. The K_1 anisotropy parameter is reduced upon replacement of Co by Ge and values of 2.8 and 2.4 MJ/m^3 have been fitted from the magnetization curves at 4 and 300 K, respectively. This clearly demonstrates that the presence of Ge not only influences the overall magnetization but also induces a strong reduction of the Co sublattice magnetocrystalline anisotropy. This large effect is typical of the influence of p elements in the YCo_5 type compounds since similar decrease of the magnetocrystalline anisotropy has been reported for Ga or Al [15,16,18,19,34].

According to our neutron diffraction investigation, substituting Ge for Co in YCo_5 led to the replacement of a Co atom exhibiting a planar anisotropy character on the 3g position by a non-magnetic Ge atom. Consequently, an increase of the overall uniaxial magnetocrystalline anisotropy could have been expected. On the contrary a reduction of the Co sublattice magnetocrystalline anisotropy is observed for $YCo_{4.5}Ge_{0.5}$. This germanium induced reduction most probably originates from the modification of the spin and orbital contributions to the Co magnetic moments upon substituting Ge for Co. Indeed, earlier reported polarized neutron diffraction experiments as well as band structure calculations have evidenced that the high anisotropy in YCo_5 is associated with an important orbital magnetic contribution, especially on the Co 2c site [33,37,40,42]. Nothing can be inferred about the orbital and spin contributions because of the inherent nature of the neutron powder diffraction techniques. Band structure calculation or polarized neutron investigation on Ge containing compounds would be useful to check this hypothesis of change of the Co spin and orbital magnetic components.

As discussed earlier, it is clear that the saturation magnetization is reduced upon Ge for Co substitution thus confirming at a macroscopic scale the reduction of the atomic magnetic moment as obtained by neutron diffraction results. The magnetization goes from 8.1 down to 5.2 μ_B/formula unit for YCo_5 and $YCo_{4.5}Ge_{0.5}$, respectively. It is worth to mention that the $YCo_{4.5}Ge_{0.5}$ compounds exhibits a significant anisotropy of the saturation magnetization. Indeed the saturation magnetization measured in the hard direction is 6 and 4% smaller than the one measured along the c-axis at 4 and 300 K, respectively. This anisotropy of the saturation magnetization is very close to the 4% reported from high magnetic field investigation of the YCo_5 single crystal [39,40].

4. Conclusions

In summary, we report on the crystal and magnetic features of the $YCo_{4.5}Ge_{0.5}$ phase. Ge for Co substitution preserves the $CaCu_5$-type crystal structure but increases slightly the unit cell. This expansion of the unit cell is more pronounced along the c-axis than in the basal plane since the c/a ration is increasing upon Ge for Co substitution. The thermal expansion of the lattice occurs mostly in the basal plane whereas the c-axis does not expand much below 200 K. A preferential occupation of Ge atoms for the 3g site is demonstrated by means of powder neutron diffraction investigations. The effects of the Ge substitution on the magnetic properties are drastic. We have evidenced a dramatic decrease of the mean Co magnetic moment, the saturation magnetization and the Curie temperature. The crystal structure investigation revealed that no dumbbell pairs are observed in $YCo_{4.5}Ge_{0.5}$ unlike what has been reported for the YCo_5 homologue.

In the $YCo_{4.5}Ge_{0.5}$ phase, the Co sublattice presents a reduced magnetocrystalline anisotropy comparison with that of the YCo_5 compound. An anisotropy parameter of 2.8 MJ/m^3 has been determined at 4 K. The large magnetocrystalline anisotropy observed at 4 K for $YCo_{4.5}Ge_{0.5}$ phase is preserved at room temperature.

Acknowledgement

The authors would like to thank the Institut Laue Langevin for the use of neutron diffraction facilities and Maria Krautz for her help in part of the work.

References

[1] K.J. Strnat, in: E.P. Wohlfarth, K.H.J. Buschow (Eds.), Ferromagnetic Materials, vol. 4, 131th ed., Elsevier Science, North-Holland, Amsterdam, 1988.
[2] K.H.J. Buschow, Rep. Prog. Phys. 40 (1977) 1179.
[3] E. Burzo, A. Chelkowski, H.R. Kirchmayr, Magnetic Properties of Metals, vol. 19, subvol. d2, 248th ed., Springer-Verlag, 1990, Landolt-Börnstein.
[4] R. Lemaire, Cobalt 32 (1966) 132.

[5] H. Rosner, D. Koudela, U. Schwartz, A. Handstein, M. Hanfland, I. Opahle, K. Kopernik, M.D. Kuz'min, K.-H. Muller, J.A. Mydosh, M. Richter, Nat. Phys. 2 (2006) 469.
[6] D. Koudela, U. Schwartz, H. Rosner, U. Burkhardt, A. Handstein, M. Hanfland, M.D. Kuz'min, I. Opahle, K. Kopernik, K.-H. Muller, M. Richter, Phys. Rev. B 77 (2008) 024411.
[7] M.D. Kuz'min, Y. Skourski, D. Eckert, M. Richter, K.-H. Muller, K.P. Skokov, I.S. Tereshina, Phys. Rev. B 70 (2004) 172412.
[8] Y. Skourski, M.D. Kuz'min, K.P. Skokov, M. Richter, D. Eckert, I.S. Tereshina, K.-H. Muller, J. Magn. Magn. Mater. 290–291 (2005) 435.
[9] G.I. Miletic, Z. Blazina, J. Solid State Chem. 180 (2007) 604.
[10] S. Yehia, S.H. Aly, A.E. Aly, Comp. Mater. Sci. 41 (2008) 482.
[11] P. Larson, I.I. Mazin, J. Magn. Magn. Mater. 264 (1) (2003) 7.
[12] I. Opahle, M. Richter, M.D. Kuz'min, U. Nitzche, K. Kopernik, L. Schramm, J. Magn. Magn. Mater. 290–291 (2005) 374.
[13] C.V. Thang, P.E. Brommer, J.P. Colpa, E. Brück, A.A. Menovsky, N.P. Thuy, J.J.M. Franse, J. Alloys Compd. 245 (1996) 100.
[14] C. Chacon, O. Isnard, J. Solid State Chem. 154 (2000) 242.
[15] H. Ido, W.E. Wallace, T. Suzuki, S.F. Chang, V.K. Sinha, S.G. Sankar, J. Appl. Phys. 67 (9) (1990) 4638.
[16] H. Ido, K. Konno, T. Ito, S.F. Chang, S.G. Sankar, W.E. Wallace, J. Appl. Phys. 69 (8) (1991) 5551.
[17] A.T. Pedziwiatr, S.Y. Jiang, W.E. Wallace, E. Burzo, V. Pop, J. Magn. Magn. Mater. 66 (1987) 69.
[18] C. Zlotea, O. Isnard, J. Alloys Compd. 346 (2002) 29–37.
[19] C. Zlotea, O. Isnard, J. Magn. Magn. Mater. 253 (2002) 118–129.
[20] N. Coroian, V. Klosek, O. Isnard, J. Alloys Compd. 427 (2007) 5–10.
[21] V. Klosek, C. Zlotea, O. Isnard, J. Phys. Condens. Matter 15 (2003) 8327.
[22] C. Zlotea, O. Isnard, J. Phys. Condens. Matter 14 (2002) 10211–10220.
[23] C. Chacon, O. Isnard, J. Phys. Condens. Matter 13 (2001) 5841–5851.
[24] C. Zlotea, C. Chacon, O. Isnard, J. Appl. Phys. 92 (2002) 7382–7388.
[25] J. Rodriguez Carjaval, Physica B 192 (1993) 55.
[26] V.F. Sears, Neutron News 3 (1992) 26.
[27] L.B. McCusker, R.B. Von Dreele, D.E. Cox, D. Louer, P. Scardi, J. Appl. Cryst. 32 (1999) 36.
[28] J.C. Picoche, M. Guillot, A. Marchand, Physica B 155 (1989) 407–414.
[29] N. Coroian, Ph.D. thesis, Université Joseph Fourier Grenoble, 2008.
[30] V. Klosek, C. Zlotea, O. Isnard, Physica B 350 (Suppl. 1) (2004) E155.
[31] J. Laforest, Université de Grenoble, 1981.
[32] C.V. Colin, O. Isnard, J. Magn. Magn. Mater. (2009) 047, doi:10.1016/j.jmmm.2009.06.
[33] J. Schweizer, F. Tasset, J. Phys. F: Met. Phys. 10 (1980) 2799.
[34] O. Moze, L. Pareti, A. Paoluzi, K.H.J. Buschow, Phys. Rev. B 53 (1996) 11550.
[35] C. Chacon, O. Isnard, J. Appl. Phys. 89 (2001) 71.
[36] H. Mayot, O. Isnard, Z. Arnold, J. Kamarad, J. Phys. Condens. Matter 20 (2008) 135207.
[37] J. Deportes, D. Givord, J. Schweizer, F. Tasset, IEEE Trans. Magn. 12 (1976) 1000.
[38] R.L. Streever, Phys. Rev. B 19 (1979) 2704.
[39] J.M. Alameda, D. Givord, R. Lemaire, Q. Lu, J. Appl. Phys. 52 (1981) 2079.
[40] J.M. Alameda, D. Givord, R. Lemaire, Q. Lu, S.B. Palmer, F. Tasset, J. Phys. C7 43 (1982) 133.
[41] O. Isnard, S. Miraglia, M. Guillot, D. Fruchart, J. Appl. Phys. 75 (1994) 5988.
[42] L. Steinbeck, M. Richter, H. Eschrig, Phys. Rev. B 63 (2001) 184431.